

Detection and identification of explosive RDX by THz diffuse reflection spectroscopy

Hai-Bo Liu, Yunqing Chen

Center for Terahertz Research, CII 9009, Rensselaer Polytechnic Institute, Troy, NY 12180
liuhb@rpi.edu, cheny8@rpi.edu

Glenn J. Bastiaans

Intelligent Optical Systems, Inc., Torrance, CA 90505

X.-C. Zhang

Physics Department, Rensselaer Polytechnic Institute, Troy, NY 12180
zhangxc@rpi.edu

Abstract: The reflection spectrum of the explosive RDX was acquired from a diffuse reflection measurement using a THz time-domain spectroscopy system in combination with a diffuse reflectance accessory. By applying the Kramers-Kronig transform to the reflection spectrum, the absorption spectrum (0.2-1.8 THz) was obtained. It agrees with the result from a transmission measurement and distinguishes RDX from other materials. The effect of the reference spectrum was examined by using both a Teflon pellet and a copper plate as references. The strong absorption of RDX at 0.82 THz allowed it to be identified by the diffuse reflection measurement even when the RDX sample was covered with certain optically opaque materials. Our investigation demonstrates that THz technique is capable of detecting and identifying hidden RDX-related explosives in a diffuse reflection mode, which is crucial for the standoff detection in the real world applications.

©2006 Optical Society of America

OCIS codes: (300.6270) Spectroscopy, far infrared; (120.5700) Reflection

References and links

1. M. C. Kemp, P. F. Taday, B. E. Cole, J. A. Cluff, A. J. Fitzgerald and W. R. Tribe, "Security applications of terahertz technology," in *Terahertz for Military and Security Applications*, R. J. Hwu and D. L. Woolard, eds, Proc. SPIE **5070**, 44-52 (2003).
2. Y. Chen, H. Liu, Y. Deng, D. Veksler, M. Shur, X.-C. Zhang, D. Schauki, M. J. Fitch and R. Osiander, "Spectroscopic characterization of explosives in the far infrared region," in *Terahertz for Military and Security Applications II*, R. J. Hwu and D. L. Woolard, eds, Proc. SPIE **5411**, 1-8 (2004).
3. K. Yamamoto, M. Yamaguchi, F. Miyamaru, M. Tani, M. Hangyo, T. Ikeda, A. Matsushita, K. Koide, M. Tatsuno and Y. Minami, "Noninvasive inspection of C-4 explosive in mails by terahertz time-domain spectroscopy," *Jpn. J. Appl. Phys.* **43**, 414-417 (2004).
4. F. Huang, B. Schulkin, H. Altan; J. F. Federici, D. Gary, R. Barat, D. Zimdars, M. Chen and D. B. Tanner, "Terahertz study of 1,3,5-trinitro-s-triazine by time-domain and Fourier transform infrared spectroscopy," *Appl. Phys. Lett.* **85**, 5535-5537 (2004).
5. M. R. Scarfi, M. Romanò, R. Di Pietro, O. Zeni, A. Doria, G. P. Gallerano, E. Giovenale, G. Messina, A. Lai, G. Campurra, D. Coniglio and M. D' Arienzo, "THz exposure of whole blood for the study of biological effects on human lymphocytes," *J. Biol. Phys.* **29**, 171-177 (2003).
6. R. H. Clothier and N. Bourne, "Effects of THz exposure on human primary keratinocyte differentiation and viability," *J. Biol. Phys.* **29**, 179-185 (2003).
7. Y. C. Shen, T. Lo, P. F. Taday, B. E. Cole, W. R. Tribe and M. C. Kemp, "Detection and identification of explosives using terahertz pulsed spectroscopic imaging," *Appl. Phys. Lett.* **86**, 241116 (2005)

8. F. M. Mirabella, *Modern Techniques in Applied Molecular Spectroscopy*, (John Wiley & Sons, 1998), Chap. 5.
9. Q. Wu, M. Litz, and X.-C. Zhang, "Broadband detection capability of ZnTe electro-optic field detectors," *Appl. Phys. Lett.* **68**, 2924-2926 (1996).
10. Y. C. Shen, P. C. Upadhy, H. E. Beere, E. H. Linfield, A. G. Davies, I. S. Gregory, C. Baker, W. R. Tribe and M. J. Evans, "Generation and detection of ultrabroadband terahertz radiation using photoconductive emitters and receivers," *Appl. Phys. Lett.* **85**, 164-166 (2004)
11. Y. Chen, H. Liu, Y. Deng, D. Schauki, M. J. Fitch, R. Osiander, C. Dodson, J. B. Spicer, M. Shur and X. C. Zhang, "THz spectroscopic investigation of 2,4-dinitrotoluene," *Chem. Phys. Lett.* **400**, 357-361 (2004).
12. S. Nashima, O. Morikawa, K. Takata and M. Hangyo, "Measurement of optical properties of highly doped silicon by terahertz time domain reflection spectroscopy," *Appl. Phys. Lett.* **79**, 3923-3925 (2001).
13. M. Khazan, R. Meissner and I. Wilke, "Convertible transmission-reflection time-domain terahertz spectrometer," *Rev. Sci. Instrum.* **72**, 3427-3430 (2001).
14. A. Pashkin, M. Kempa, H. Nemeč, F. Kadlec and P. Kuzel, "Phase-sensitive time-domain terahertz reflection spectroscopy," *Rev. Sci. Instrum.* **74**, 4711-4717 (2003).
15. E. M. Vartiainen, Y. Ino, R. Shimano, M. Kuwata-Gonokami, Y. P. Svirko and K.-E. Peiponen, "Numerical phase correction method for terahertz time-domain reflection spectroscopy," *J. Appl. Phys.* **96** (8), 4171-4175 (2004).
16. F. Stern, *Solid State Physics*, edited by F. Seitz and D. Turnbull (Academic Press, Inc., New York, 1963) **15**, 299.
17. F. M. Mirabella, *Modern Techniques in Applied Molecular Spectroscopy*, (John Wiley & Sons, 1998), Chap. 3.
18. M. van Exter, C. Fattinger and D. Grischkowsky, "Terahertz time-domain spectroscopy of water vapor," *Opt. Lett.*, **14**, 1128-1130 (1989).
19. T. Yuan, H. Liu, J. Xu, F. Al-Douseri, Y. Hu and X.-C. Zhang, "Terahertz time-domain spectroscopy of atmosphere with different humidity," in *Terahertz for Military and Security Applications*, R. J. Hwu and D. L. Woolard, eds, *Proc. SPIE* **5070**, 28-37 (2003).

1. Introduction

Many commonly-used solid-state explosives and related compounds (ERCs), including RDX (hexahydro-1,3,5-trinitro-1,3,5-triazine), TNT (2,4,6-trinitrotoluene), HMX (tetramethylene tetranitramine), PETN (pentaerythritol tetranitrate), and DNT (dinitrotoluene), have spectral fingerprints in the range of 0.1-2.0 THz [1-4]. Most of them arise from the phonon modes of these polycrystalline explosive materials. THz (far-infrared) waves in this range can penetrate through many commonly-used nonpolar dielectric materials such as paper, plastic, leather, wood, and ceramic. In addition, THz waves have low photon energies (4 meV for 1 THz, one million times weaker than X-ray photons) and will not cause harmful photoionization in biological tissues [5, 6]. Therefore, as a potential sensing and imaging modality, THz radiation is considered a safe method for the operators and targets. Due to these advantages, THz technology is a competitive method for inspecting hidden explosives. Several groups have applied THz time-domain spectroscopy (THz-TDS) for explosives detection in transmission mode [1-4]. However, for real-field applications, reflection measurements are preferred since most bulky targets are impossible to measure in a transmission mode, in which the targets will attenuate the incident THz waves completely. In addition, reflection spectroscopy, especially diffuse reflection spectroscopy, is more applicable for standoff detection than transmission methods. Since in standoff detection, individuals and vital assets should be outside the zone (e.g., in a distance of > 10 m) of severe damage of an explosive detonation. Detection of RDX by THz specular reflection spectroscopy has been demonstrated recently [7]. However, a more realistic standoff sensing mode, detection and identification of RDX by diffusely reflected THz waves has not been reported previously. This paper presents our measurements and analysis of diffuse reflection spectroscopy of exposed and covered RDX.

When THz waves illuminate a flat sample surface, the reflected THz beam with a reflection angle the same as the incident angle can be theoretically treated using the Fresnel equations and it is called specular Fresnel reflection. In a real world scenario, the targets are usually not flat and not aligned normal to the THz beam. Thus the direction of the specular

reflection is hard to determine. It is more feasible to detect the diffusely reflected THz waves. Fig. 1 schematically shows the reflection geometry consisting of both specular Fresnel reflection and diffuse Fresnel reflections [8]. Since the sample surface is not optically flat for THz waves, the diffuse Fresnel reflections are caused by some tiny planes statistically distributed at all angles, as shown in Fig. 1. Although the reflected THz waves from these small surfaces undergo specular reflection, the collected THz waves are seemingly the diffuse reflected parts with respect to the macroscopic sample surface. Therefore, we use the term “diffuse Fresnel reflection”. Since most of the sample surface is parallel with the macroscopic sample surface, reflection from that portion of the surface is dominant and is termed specular Fresnel reflection. However, studying the small amount of diffuse Fresnel reflection is more applicable than specular reflection for standoff detection of bulky explosives in the real world where target orientation with respect to the irradiation beam is randomly distributed.

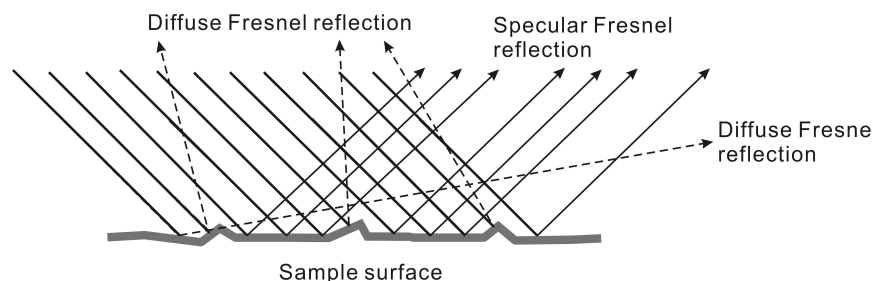


Fig. 1. Rough sample surface results in diffuse reflection. Specular reflection, indicated by the solid lines, has a reflection angle equal to the incident angle. Diffuse reflections, denoted by the dashed lines, have reflection angles that are independent of the incident angle.

RDX is a highly explosive compound with both military and civilian applications. C-4, a plastic explosive containing 91% RDX by weight can be easily molded and is barely detectable by X-ray imaging. New non-contact and nondestructive techniques, such as THz spectroscopy, need to be developed for effective detection of explosives like C-4.

The THz-TDS generates and detects picosecond THz pulses by a coherent and time-gated method using near-infrared femtosecond laser pulses [9]. It is able to cover a frequency range from about 0.2 to 15 THz with a high signal-to-noise ratio (SNR), ideal for THz spectroscopic applications [10]. Coherent and time-gated detection offers a high dynamic range. In our investigation, dynamic range of the measured THz power reaches up to 60 dB (the ratio of the highest THz signal to the noise level in the THz power spectrum) for a THz-TDS system with a bandwidth of 0.1-2 THz. This advantage makes THz-TDS an effective technique for chemical sensing and identification.

The objective of this study is to apply THz-TDS to investigate diffuse reflection spectroscopy of explosives using RDX as a model compound. Our investigation implies that THz diffuse reflection spectroscopy has the potential for the standoff detection and identification of explosives concealed in packages or under clothing.

2. Samples

RDX acetone solution (purity > 99%) was purchased from AccuStandard, USA. Solid-state RDX were recrystallized from the solution. Two commonly-used materials without THz absorption features, polyethylene and flour, were also tested to compare with RDX. Powdered materials of RDX, Teflon, polyethylene and flour were grounded to fine particles below 50 μm in diameter. The pure powder of each material was compressed into a pellet with a thickness of ~ 2 mm and a diameter of 13 mm. A Teflon pellet and a copper plate were used in the experiment as references. The surfaces of pellet samples and copper plate were not perfectly flat for THz waves. The approximate length of the surface variations was < 50 μm

for the pellet sample and $< 10 \mu\text{m}$ for the copper plate. As a result, small parts of THz waves can be diffusely reflected from the samples.

3. Experimental methods

Fig. 2 depicts the schematic diagram of a THz-TDS setup coupled with a diffuse reflectance accessory (Specac, UK). THz pulses were generated by an 800 nm femtosecond laser (Mai Tai, Spectra Physics, USA) with a pulse duration of ~ 80 fs, repetition rate of 80 MHz, and average power of 800 mW. The laser beam was split into pump and probe beams. The chopped pump beam (~ 300 mW) was focused on a p-type InGaAs crystal to generate THz pulses. The emitted THz pulses were collimated and focused by a pair of parabolic mirrors, then propagated through the diffuse reflectance accessory wherein sample was placed. The output THz pulses were subsequently collected and focused using another pair of parabolic mirrors onto a 2 mm-thick $\langle 110 \rangle$ ZnTe crystal, in which the probe beam detected the THz field by electro-optic sampling [9]. The THz spectrum in the range of 0.2-1.8 THz was obtained by applying a fast Fourier transform to the THz waveform with a 4-times zero-padding. The achieved real spectral resolution was 100 GHz.

In the diffuse reflectance accessory, the THz beam was focused on the sample by an off-axis ellipsoidal mirror and the beam size at the focal point is about 2 mm. The incident angles are around 45° . A quarter of all the diffusely reflected THz radiation was collected by the second off-axis ellipsoidal mirror. The unique configuration of this accessory deflected the specular reflection away from the collecting ellipsoidal mirror. The focal length of the two ellipsoidal mirrors was ~ 5 cm. About 1/10000 of incident THz power was collected and detected in the diffuse reflection measurements.

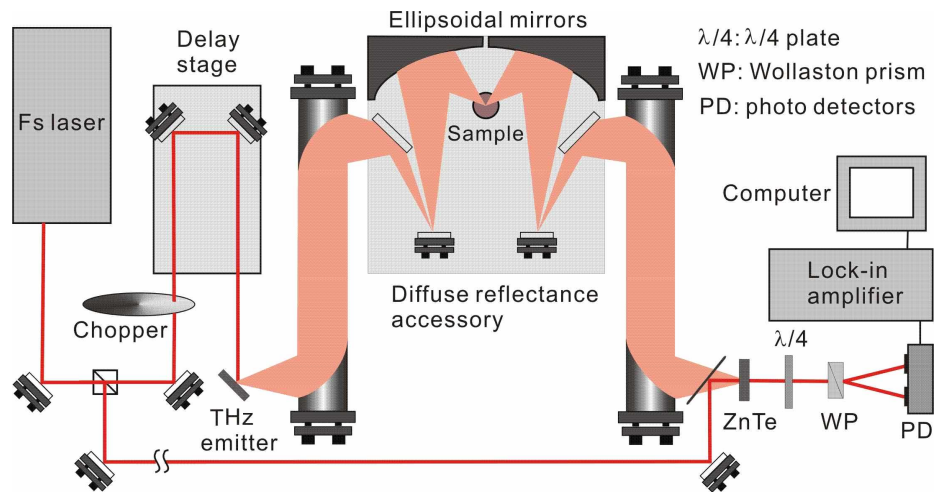


Fig. 2. A planform of THz-TDS with a diffuse reflectance accessory.

4. Theoretical background

THz-TDS can be used to measure both the phase and the amplitude of THz waves. Therefore, the complex refractive index of a sample can be obtained without using the Kramers-Kronig (K-K) transform [11]. In a reflection mode, since the phase of the THz pulse depends on the position of the reflected surface, an accurate phase measurement requires a reference reflector exactly in the same position as the sample. The reference reflector should have a very similar surface morphology as the sample as well. In real-world applications, this match is hard to realize. Thus for the samples that are not optically smooth for THz waves, the retrieval of phase information from the time-domain signal is difficult for reflection measurements. Although several techniques have been proposed to minimize this phase error [12-15], it still

remains a bottleneck for THz-TDS in specular reflection geometry. Diffuse reflection is even more complicated than specular reflection. Retrieval of the phase has proved to be a difficult problem in our investigation. Considering this difficulty, we discarded phase information obtained in the reflection measurement. The K-K transform was used to obtain the absorption spectrum from the measured reflection spectrum.

If the complex refractive index of the sample is $N = n + ik$, the amplitude reflectivity r and power reflectivity R are expressed as:

$$r = \sqrt{R}e^{i\theta} \quad (1)$$

θ is the phase shift defined in terms of the Fresnel reflection coefficient.

The K-K dispersion relationship is used to determine the spectrum of the complex refractive index from the specular reflection spectrum in many conventional spectroscopy technologies [16]. \sqrt{R} and θ in Eq. (1) are mutually correlated according to the K-K equation:

$$\theta(\nu_0) = \frac{2\nu_0}{\pi} P \int_0^{\infty} \frac{\ln \sqrt{R(\nu)}}{\nu^2 - \nu_0^2} d\nu \quad (2)$$

where P is related to the Cauchy principal value. Using this equation, the phase change at any frequency ν can be calculated when the power reflectivity $R(\nu)$ is obtained. Then the real and imaginary parts of the complex refractive index are calculated via the following formulas:

$$n = \frac{1 - R}{1 + R - 2\sqrt{R} \cos \theta} \quad (3)$$

$$k = \frac{2\sqrt{R} \sin \theta}{1 + R - 2\sqrt{R} \cos \theta} \quad (4)$$

The absorbance can be calculated as:

$$\alpha = \frac{4\pi\nu k}{c} \quad (5)$$

The real part of the refractive index can be calculated in terms of Eq. (3). It reflects the similar spectral characteristics as the imaginary part of the refractive index based on K-K relationship. Since the absorption spectrum (imaginary part) is commonly used in sensing applications, the real part of the refractive index was not studied in this investigation. Strictly, the reflection spectrum needs to be measured at near-normal incidence to use the above equations. In our diffuse reflection measurements, incident angles have a range at around 45° (from ~35° to ~55°). To our best knowledge, there is no completely sound theory for retrieving the absorption spectrum from the diffuse reflection data obtained in this investigation. Utilizing the K-K transform and Fresnel equation to calculate the absorption spectrum in this case was an approximation. The absorption intensity obtained from Eq. (4) and (5) has an arbitrary unit, nevertheless this relative absorption spectrum provides us sufficient fingerprint information for sensing explosives.

5. Experimental results and discussion

The diffusely reflected THz pulses from the RDX and from the Teflon pellet surfaces were measured in a chamber purged with nitrogen to avoid the effect of water vapor absorptions in ambient air. The measured amplitude of diffusely reflected THz waves was about 1/100 (1/10000 for the THz power) of that of the incident THz beam. Therefore, the dynamic range for the power spectrum of diffusely reflected THz waves was approximately 20 dB (60 dB for non-reflection freepath measurements as mentioned previously). For each sample, we measured 10 different spots on the sample surface to reduce the surface effect. THz spectrum was obtained by applying the fast Fourier transforms (FFT) to each THz pulse waveform. The

averaged reflected THz spectrum was calculated from the 10 spectra. The relative reflection spectrum of RDX can be calculated as $R(\nu)/R_0(\nu)$, which is the ratio of the reflected THz power of RDX, $R(\nu)$, to that of Teflon, $R_0(\nu)$, as plotted in Fig. 3(a). The relative reflection spectra of polyethylene and flour are also presented for comparison. Because RDX is dispersive and absorptive in the THz band, its reflection spectrum differs from those of polyethylene and flour. After the K-K transform, the absorption spectra of RDX, polyethylene and flour were acquired using Eq. (2), (4) and (5) and are plotted in Fig. 3(b). Fig. 3(c) displays a direct comparison between the results of RDX from the transmission measurement and diffuse reflection measurement. The strong absorption peak at 0.82 THz and the three other relatively weak absorption peaks at 1.05, 1.35 and 1.55 THz can be well identified by the diffuse reflection measurement, and they agree closely with the transmission measurement. Our transmission spectrum is in good accordance with the results previously reported [3, 4].

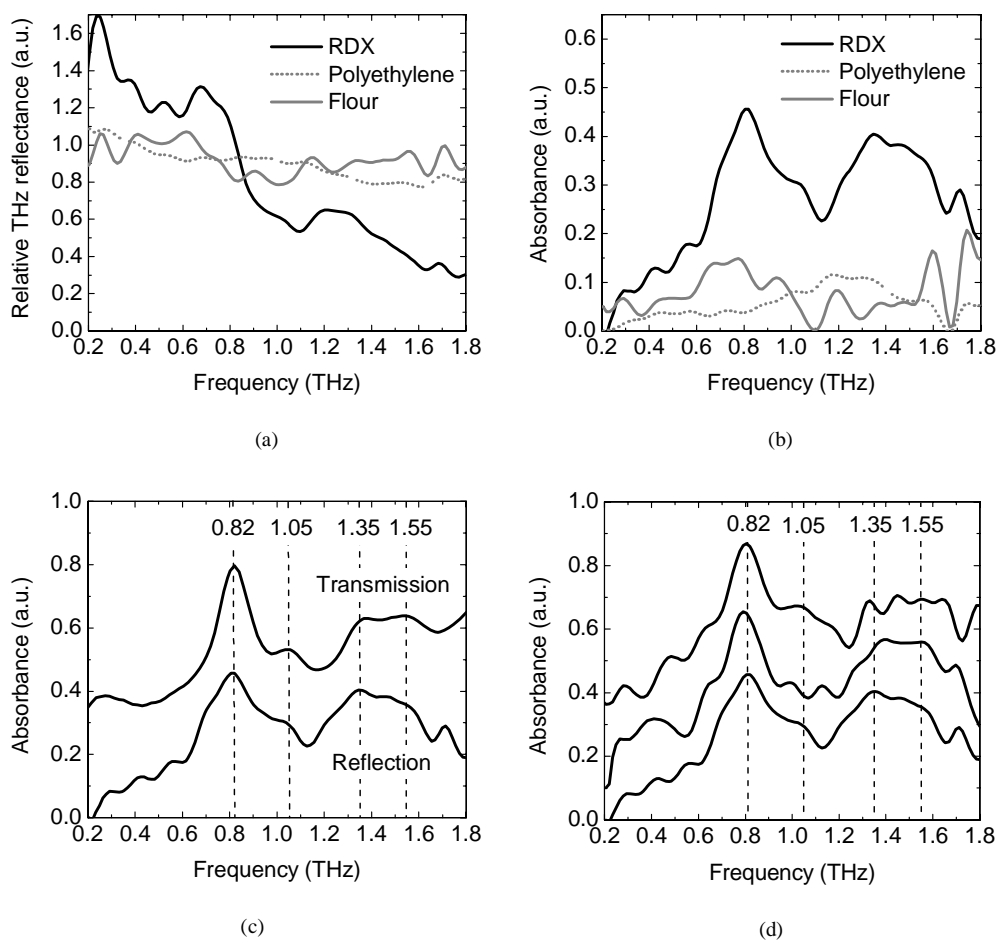


Fig. 3. (a) Relative power reflection spectra of RDX, polyethylene and flour, the diffuse spectrum of Teflon was used as reference; (b) Absorption spectra of RDX, polyethylene and flour from the K-K transform of the reflection spectra; (c) The comparison between the absorption spectra from the transmission measurement (upper curve) and diffuse reflection measurement (bottom curve); (d) Absorption spectra of 3 different RDX samples. All the measurements were conducted in nitrogen atmosphere to avoid the effect of water vapor absorption in ambient air. The dashed lines indicate the absorption peak positions.

There are some small spectral variations in the obtained absorption spectra of polyethylene and flour as shown in Fig. 3(b). This finding differs from the result obtained from the transmission measurements of polyethylene and flour, which have no THz absorption features. We attribute the discrepancy to the surface difference between the sample (polyethylene or flour) and reference (Teflon). Because of the phase shift in the THz waves that occurs upon reflection, the mean-square electric fields present near an interface are dependent on the polarization of the incident radiation. This situation gives rise to a surface effect, often referred to as *surface selection rule*, reflecting the information on the structural orientation of the sample surface [17]. Changes in reflectivity due to these surface differences can result in a distortion in the band shape and a shift of the obtained absorption maximum compared with the result from a transmission measurement. However, predictions of band shapes are hindered by a complicated interplay of mean-square electric fields, angles of incidence, polarizations, and the reflectivities between different phases in a stratified medium. On the other hand, as we see from Fig. 3(b), these distortions or spectral variations are relatively small compared with some intense absorption features in the RDX absorption spectra. These results reveal that THz diffuse reflection spectroscopy can distinguish RDX from other materials that have no THz fingerprints, such as polyethylene and flour.

In additional work, the measured phase was used to acquire the absorption spectrum using Eq. (4) and (5) instead of using Eq. (2) to calculate the phase from the K-K relationship. However, because of the misplacement phase error in the diffuse reflection measurement, the absorption spectrum obtained (not shown in the paper) did not contain any RDX fingerprints.

To test the reliability of the results shown in Fig. 3(c), we measured three different RDX pellet samples that were prepared separately and assumed to have small differences in surface morphology. The obtained absorption spectra are plotted in Fig. 3(d). Although the three weak absorption peaks could not be repeated well because the surface effect described above, the strong one at 0.82 THz could be well identified in each sample. Detecting a spectral fingerprint at 0.82 THz of RDX is especially preferred on account of atmospheric attenuation. The atmospheric attenuation at 0.82 THz is relative low compared with that in the frequency above 1.0 THz, since 0.82 THz is away from the closest absorption lines of water vapor at 0.75 and 0.99 THz. The following results measured in the atmosphere (Fig. 5) confirm this.

In most of the reflection spectroscopic investigations, a metal surface or mirror is usually used as a reference. We used a Teflon pellet instead of a metal surface because of the similarity between the RDX and Teflon pellets, which were both compressed from powders. In order to compare the influences from the different references, we also chose the reflection spectrum of a metal surface as the reference to obtain the absorption spectrum of RDX. A copper plate was chosen in our investigation, and the measurement was also conducted in nitrogen. Fig. 4 presents the comparison between the results of using Teflon and copper as references. Four absorption peaks still are observed in the case of using copper as reference, although there is some band shape change close to the absorption maximum at 0.82 THz. The band shape change can also be explained by the surface difference between the RDX pellet and copper plate. The RDX pellet surface is different from the copper plate surface, and more similar to the Teflon pellet surface. However, this band shape change does not affect the identification of the absorption fingerprints, as shown in Fig. 4. Obtaining the same absorption fingerprints using different references is significant for real world applications. Our result indicates that THz technology can be a feasible method for the real-field detection of RDX by using one or more surrounding materials (which have no THz absorption features) as references.

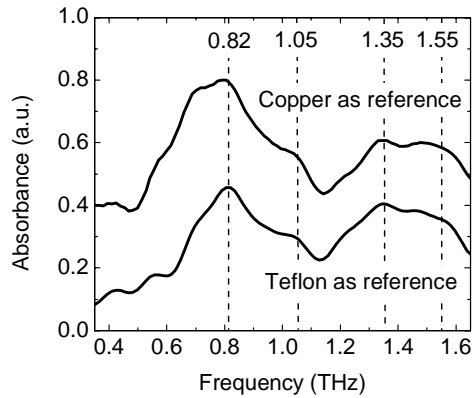


Fig. 4. Absorption spectra of RDX from the K-K transform of the reflection spectra using Teflon as reference and copper as reference respectively. The dashed lines indicate the absorption peak positions.

The THz technology combines two advantages for the detection of hidden explosives: explosives have THz fingerprints and many commonly-used nonpolar dielectric materials have low absorption for THz waves. In order to demonstrate both capabilities, we investigated the THz diffuse reflection spectroscopy of RDX under covering materials. The RDX samples were covered with four different barrier materials, paper (thickness: ~ 0.05 mm, white), polyethylene sheet (~ 0.1 mm, black), leather (~ 0.3 mm, yellow) and polyester cloth (~ 0.4 mm, green), which were all opaque for visible light. The measurements were conducted in the atmosphere (with a relative humidity of $\sim 20\%$ at 25°C) instead of nitrogen and the whole path length of THz waves was ~ 110 cm. The absorption spectra obtained from the K-K transform are plotted in Fig. 5. In the atmosphere, water vapor absorptions affect the measurements, especially in the range beyond 1.0 THz, since there are many water vapor absorption bands in the THz range, with absorption maximums at 0.56, 0.75, 0.99, 1.10, 1.11, 1.16, 1.21, 1.22, 1.41, 1.60, 1.66, and 1.71 THz [18, 19]. The strong water vapor absorptions reduce the SNR in these bands and lead to band distortions or artificial spikes in the absorption spectrum of RDX. Especially in the range close to 1.66 and 1.71 THz, the water vapor absorption almost attenuates the THz signal completely, resulting in the big artificial spikes shown in Fig. 5(a). In addition, the barrier materials also lead to the distorted spectral band shapes and the shifts of absorption maximums. For the paper cover, because it is relatively thin and its surface is smooth, the obtained absorption spectrum is not distorted too much and in good agreement with the result without cover. For the other three covers, the rough surfaces and inhomogeneous thicknesses of the covers cause the distorted reflection spectra and therefore the distorted absorption spectra of RDX after the K-K transform. Because of both water vapor absorptions and covering effects, most of the weak absorption features of RDX can not be identified, and there are even artificial features. However, the absorption peak at about 0.82 THz is always observed behind all barriers in the atmosphere. This demonstrates the THz technique as an applicable tool for detecting hidden explosives, such as C-4 under clothing or inside package in diffuse reflection geometry.

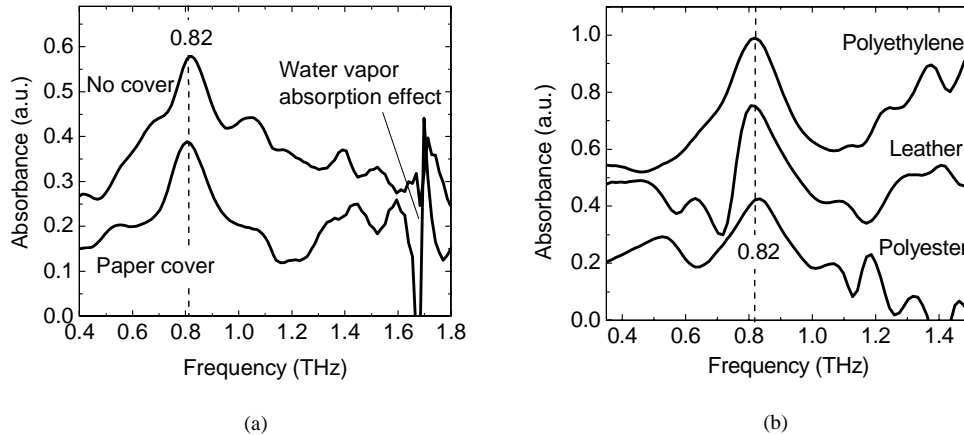


Fig. 5. (a) A comparison between the absorption spectra of RDX obtained from the diffuse reflection measurements when RDX was bare and was covered with paper; (b) Absorption spectra of RDX obtained from the diffuse reflection measurements under different covers. Upper curve: polyethylene sheet cover; middle curve: leather cover; bottom curve, polyester cloth cover. The dashed lines indicate the absorption peak positions.

6. Conclusion

In summary, we measured the diffuse reflection spectrum of a RDX pellet by using a THz-TDS system coupled with a diffuse reflectance accessory. Referenced to the reflection spectra of either Teflon or copper, the relative reflection spectrum of RDX was calculated. The absorption spectrum obtained from the K-K transform agrees with that of the transmission measurement. The repeatability was good, especially for the strong absorption at 0.82 THz. The reflection spectra and corresponding absorption spectra of two materials, polyethylene and flour were also tested for comparison. THz diffuse reflection spectroscopy could distinguish the RDX from the polyethylene and flour. In the atmosphere, the water vapor absorptions affected the obtained THz spectrum, especially in the range above 1.0 THz. When the RDX sample was covered with some optically opaque materials, the THz absorption fingerprint at 0.82 THz was still well identified by the diffuse reflection measurement. Our investigation has demonstrated that THz techniques are promising for the detection of RDX-related explosives hidden inside clothing or package in the diffuse reflection configuration, which is significant for the standoff detection and identification in real world applications.

Acknowledgments

This work is supported by the U.S. Army Research Office under the MURI project contract/grant number DAAD190210255, and HSARPA SBIR grant through Intelligent Optical Systems, Inc.